Retinal HDR Images: Intraocular Glare and Object Size

John J. McCann and Alessandro Rizzi; McCann Imaging, Belmont, MA 02478, USA and Dipartimento di Tecnologie dell'Informazione, Università degli Studi di Milano, 26013 Crema (CR), Italy

Abstract

Starting from measured scene *luminances, we calculated the* retinal *luminance images of High Dynamic Range (HDR) test targets. These test displays contain 40 gray squares with a 50% average surround. In order to approximate a natural scene the surround area was made up of half-white and half-black squares of different sizes. In this way, the spatial-frequency distribution approximates a 1/f function of energy vs. spatial frequency. We compared images with 2.7 and 5.4 optical density ranges. Although the target luminances are very different, after computing the retinal image according to the CIE scatter glare formula, we have found that the retinal luminance ranges are very similar. Intraocular glare strongly restricts the range of the retinal image. Further, uniform, equiluminant target patches are spatially transformed to different gradients with unequal retinal luminances. The usable dynamic range of the display correlates with the range of retinal luminances. Observers report that appearances of white and black squares are constant and uniform, despite the fact that the retinal stimuli are variable and non-uniform. Human vision uses complex spatial processing to calculate appearance from retinal luminance arrays. Our spatial image processing increases apparent contrast with increased white area in the surround. Spatial vision counteracts glare. The spatial contrast mechanism is much more powerful when compared with retinal, rather than with target luminances. This study adds additional evidence that human vision uses spatial image processing to synthesize appearance, rather than using the array of independent retinal responses.*

Introduction

At times, research on human vision describes detailed information about the stimulus using radiometric, or photometric, measurements of the scene, or of the test target. Such studies analyzing human image processing need to consider the light distribution of the image falling on the retina after intraocular scatter.

High Dynamic Range (HDR) imaging is a good example. HDR images capture and display a greater range of information than conventional images.[1-3] However, scene-dependent scatter in cameras, and in the human eye, controls the ranges of information and appearances. [2-8]

We studied the effects of intraocular scatter and the size of image elements with calculated retinal images. We used van den Berg's CIE scatter standard [9-11] to calculate the image on the retina. We found large changes in spatial distribution of retinal luminances compared to target luminances. The retinal luminances changed dramatically with change in the size of target elements in the surround.

Design of Target

We measured how veiling glare affects tone scale functions that relate display luminance to appearance in HDR images. To start, we can set aside all the complexities introduced by nonuniformites in illumination. We will just study patches of light that are uniform in the target. [12]

We used a surround that is, on average, equal to the middle of the dynamic range (50% max and 50% min luminances). Further, these surround elements are made up of different size min and max blocks, spatially unevenly distributed, so that the image has energy over a wide range of spatial frequencies. It avoids the problem that simultaneous contrast depends on the relative size of the white areas and of the test patch.[13] Plots of the radial spatial frequency distribution vs. frequency approximate the 1/f distribution [14] found in natural images.

Targets Layout

Figures 1 & 2 show the layout of the min/max test target. The display subtended 15.5 by 19.1 degrees. It was divided into 20 squares, 3.4 degrees on a side. Two 0.8 degree gray patches are within each square along with various sizes of max and min blocks. The two gray square length subtends an angle approximately the diameter of the fovea. The smallest block (surrounding the gray patches) subtends 1.6 minutes of arc and is clearly visible to observers. The blocks 2x, 4x, 8x, 16x, 32x, 64x are used in the surround for each gray pair.

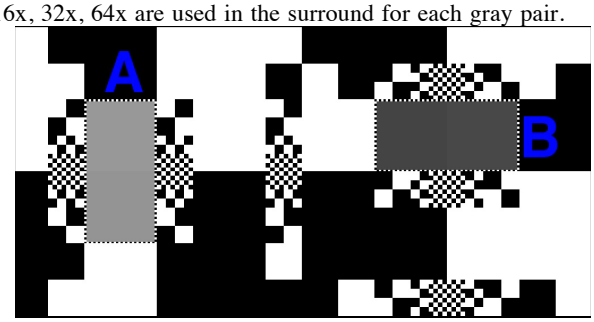

Figure 1. Magnified view of two of twenty gray pairs of luminance patches. The left half (square A) has the same layout as the right (square B), rotated 90° clockwise. Gray areas in A and B have slightly different luminances. The surrounding areas are identical except for rotation. For each size there are equal numbers of min and max blocks.

Single- and Double-Density Targets

Figure 2 shows the 4 by 5 inch film transparency (Single Density) test target. We calculated the array of retinal luminances from the array of measured uniform target luminances. The Double-Density target was the aligned superposition of two identical (Single-Density) films.[15-18]

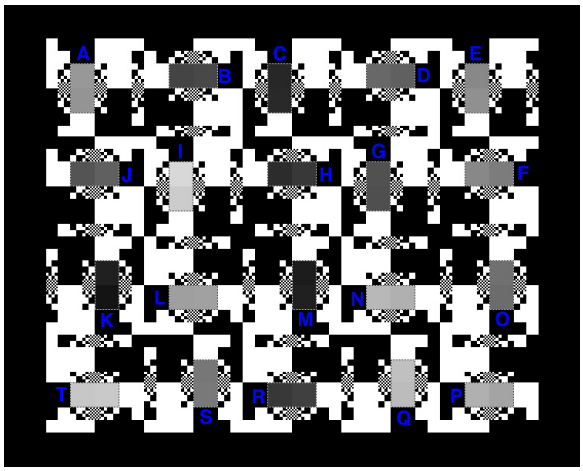

Figure 2 shows all twenty gray pairs of luminance patches. All gray pairs are close in luminance.

Two transparencies double the optical densities. [Optical Density = log10 (1/transmittance)] The whites in each transparency have an optical density (O.D.) of 0.19; the blacks have an O.D. of 2.89. The Double Density images have a min of 0.38 and a max of 5.78 O.D. (See Table 1). Both transparency configurations are backlit by 4 diffused fluorescent bulbs.

Target	Max cd/m²	Min cd/m²	Range:1	%Average cd/m²	O.D. Min	O.D. Max	O.D. Range
Single Contrast	684	1.36	501	50.01%	0.19	2.89	2.70
Double Contrast	441	0.0018	251,189	50.00%	0.38	5.78	5.40

Table 1 list the luminances and optical densities of the min and max areas in Single- and Double-Density (Contrast) displays.

Veiling glare for the Human Visual System (HVS) is a property of the luminance of each image point and the glare spread function (GSF) of the human optical system. Surrounds made up of half-max and half-min luminances have nearly the same glare properties for Single- and Double-Density test targets. The average luminance of the Single-Density target is 50.10% of the maximum luminance, from a display with a range of ~500:1. The average luminance of the Double-Density target is 50.00% of its maximum luminance, from a display with a range of ~250,000:1.[14] The effect of glare on the luminances of the gray test areas will be very nearly the same, despite the fact that the dynamic range has changed from 500:1 to 250,000:1. In other words, the black areas (min luminances) in both Single- and Double-Density targets are so low, they make only trivial contributions to glare. The white (max luminances) in both targets are almost equal and generate virtually all the glare. The layouts of both targets are constant. The physical contributions of glare are very nearly constant. By comparing the calculated retinal luminances with the appearance of these Single- and Double-Density targets, we measured the effects of constant glare on very different dynamic-range displays.[15-18]

Appearances in Single & Double Density

In order to measure the appearances of the Single and Double Density targets we asked observers to estimate the appearance of each of the 40 test squares. White was assigned to be 100; black was 1. Recent papers describe the observer estimates of appearance for Single and Double Density displays with 100%, 50%, 8% and 0% backgrounds. [13-15] The results show that there is a limited dynamic range that observers can see. The range varies with the amount of white in the background. The range increases with decreased average background whiteness. Observers report the range of appearances from white to black with the target stimuli range of 2.0 $\log_{10}$ units in a 100% white surround. When 50% of the white background is removed, the observers report that blacks are 2.3 $\log_{10}$ units darker than white. With white in only 8% of the background, the white-black range covers 2.7 $\log_{10}$ units. With 100% black background, the range overtakes 4 $\log_{10}$ units. These experiments show that the appearance of a pixel with a fixed luminance value will vary substantially with the amount of white in the background. Further, it shows only minor changes in appearance with very large changes in target dynamic range. Only grays in a black surrounds respond to increased dynamic range.[15-18]

Calculated Retinal Luminance

There are three steps in determining the luminances falling on the retina. First, we need to measure the luminance at each pixel in the target viewed by observers. Second, we need to determine the glare point spread function of human vision. Third, we need to create an efficient algorithm that can read the entire scene array and, taking into account viewing distance and other parameters, transform scene luminances to retinal luminances.

Input luminance array

The first step in the calculation is to read the digital array and use the appropriate calibration LUT to convert digit to target O.D., and then to measured luminance (cd/m^2). The lightbox has a luminance of 1059 cd/m^2. We used all the optical density measurements of white, black, gray calibration squares on the side of both transparencies to create a LUT for each target. This program reads a digit from the file sent to the film recorder, looks up the measured optical density and reduces the light box luminance by the film's corresponding % transmission value. The program reads the 0-255 value in the digital array and replaces it with the floating-point luminance value accurate over 6 log units. This accuracy is assured by the densitometer measurements of each separate single transparency against calibrated standard samples.

van den Berg's CIE scatter standard

1939 CIE meeting reported an empirical description of veiling glare estimated proportional to $1/\theta^2$, J. Vos and T. van den Berg collected a series of measurements and wrote a more recent CIE report [9] dated 1999, in which a whole set of formulas are proposed according to the desired degree of precision and other parameters like the age of the observer and the type of his/her iris pigment.

We decided to report in this paper results from the formula referred as number eight in the report [9] since it is the most complete. These calculations are described in detail in a recent paper.[17]

Applying the filter

We used Matlab© to compute the Glare Spread Function (GSF) from the CIE formula (Figure 3) to convolve it with the input image converted into luminance values.[17]

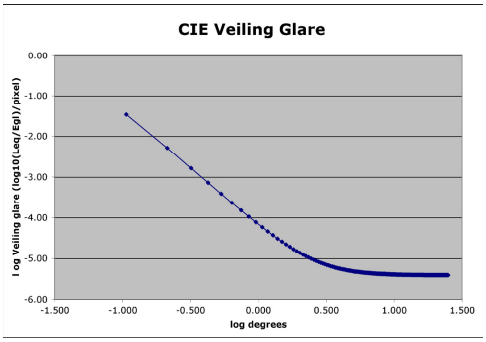

Figure 3 GSF filter plotted in log scale.

Analysis: Target vs. Retinal Luminance

The range of target luminances for the Single-Density target was 2.7 OD units. It is not possible to reproduce this range on print and conventional displays. The Double-Density target made the problem much more severe. We use a 64-pseudocolor colormap to render the target luminance range of 5.4 OD units. The maximum luminance was white and the minimum was black. The colors, in decreasing luminance, are white, yellow, green cyan, blue, magenta, red brown, and black. Rendering the range of 5.4 OD target luminances in 64 steps gives a range of 0.084 OD per individual colorbar element. We show the pseudocolor scale in the center of Figures 4-6. The color map images illustrate the substantially different ranges of luminance measured in the 2.7 OD Single-Density and 5.4 Double-Density targets.

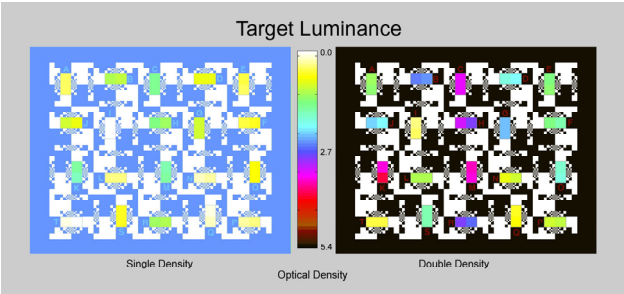

Figure 4 shows a pseudocolor rendering of target luminance. The Double-Density target has a range of 5.4 (OD); the Single Density has a 2.7 (OD) range. The colorbar in the center identifies the color of each optical density over the range of 5.4 log units. The Single- and Double-Density targets are very different stimuli.

We used the same colormap to render the calculated retinal luminances of the Single-Density and Double-Density images (Figure 5). Unlike the Figure 4 renditions, the retinal luminances are very similar to each other. Intraocular scatter reduces the 5.4 OD dynamic range of the Double-Density target to about 2.0 log units on the retina. It is only slightly darker than the Single-Density retinal luminance array.

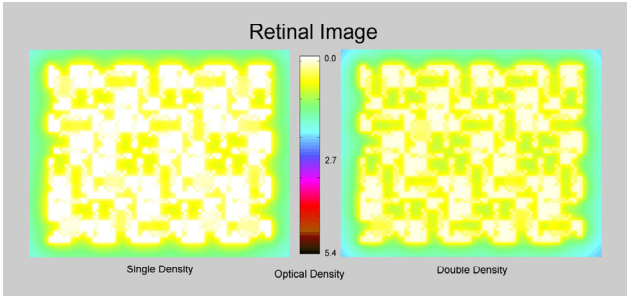

Figure 5 renders the retinal luminance using the same pseudocolor used in Figure 5. Both the Single- and Double-Density retinal ranges are roughly 2.0 (OD). The Single- and Double-Density images are very similar retinal stimuli. The DD retinal image is slightly darker (bluer corners) and the SD retinal image is slightly lighter.

The calculated retinal luminances show that intraocular glare limits the range of luminances to roughly 2.0 OD units for these 50% white targets. The white surround patches have nearly the same densities in both target and retinal luminances. The black surround squares have very different densities in the targets, but because of scatter, they are nearly the same in the range of retinal luminances. The 40 gray test patches have twice the density in the Double-Density target. That means that more squares have optical densities greater than 2.0. In other words, more than half the squares are below the limit determined by scattered light. Hence the gray test squares in the Double-Density targets show more retinal similarity. Recall that the observer data from discrimination experiments was limited to 2.3 OD range.[16]

Figure 6 shows a different colorbar rendering of retinal luminance from that in Figures 5 and 6. Here we spread the same 64-colorbar elements over only 1.0 OD, instead of 5.4 OD. Rendering the range of 1.0 OD target luminances in 64 steps gives a range of 0.0156 OD per individual colorbar element. This rendition shows the after-scatter values of the 20 pairs different gray patches in the targets. In the Single-Density target we see a range of different colors for the different transmissions. In the Double-Density target we see that intraocular scatter made many of the darker gray squares more similar.

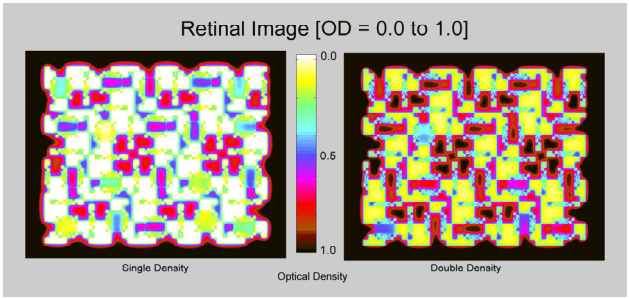

Figure 6 shows a different rendition range of retinal luminance than in Figures 5, using a new colormap on both images. To improve pseudocolor discrimination, the range of the colormap in this plot is only 1.0 (OD). This colormap rendering brings out the more subtle differences between Single- and Double-Density retinal images.

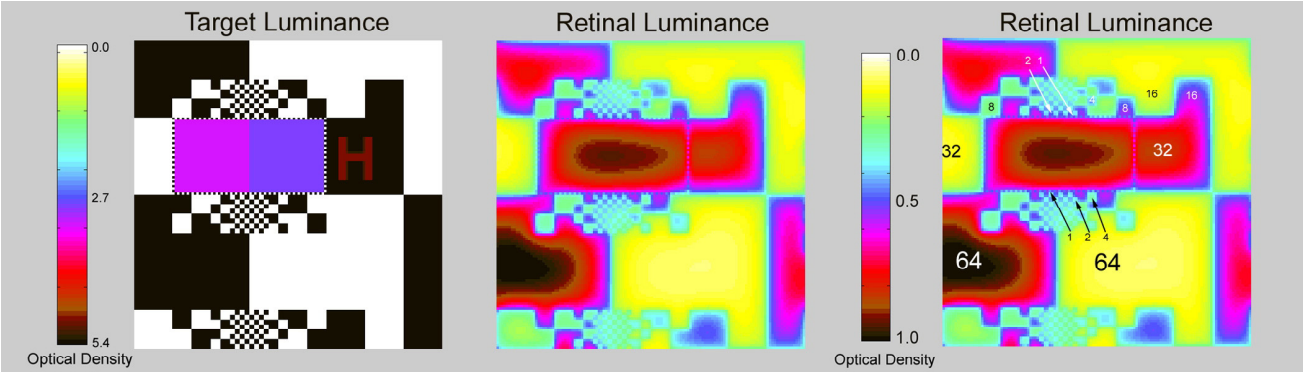

Figure 7 shows (left) the target luminance [colormap range =5.4], (center) the retinal luminance, and (right) the annotated retinal luminance using the same pseudocolor map rendition in Figures 6 [colormap range=1.0]. The annotation numbers 64,32, …, 1 show the relative sizes of sides of the white and black squares. It shows only Double-Density Area H and its surround. It illustrates the effect of intraocular scatter on different size white and black squares.

Discussion

Veiling glare from a single pixel decreases with distance away from that pixel. Figure 3 shows the falloff of scattered luminance vs. distance. The value of glare reaches an asymptote with large distances. This asymptotic value is very small, but a small contribution comes from every pixel in the image. The sum of many very small contributions is a significant number. The greater the % white in the scene, the more the amount of glare, the lower the contrast of the retinal image.

The background in these images has a range of different sizes of uniform white or black squares. Each white pixel scatters a fraction of its light into surrounding pixels. In turn, each pixel receives a distance-dependent fraction of light from all other pixels. A pixel in the center of a large white square has the highest retinal luminance because there are many surrounding white pixels that contribute a larger fraction of their scattered light. Similarly, the lowest luminance pixels are found in the center of the largest black square since it is the furthest from white pixel scatter sources. The highest ratio of retinal radiances (retinal contrast) is the ratio of the center pixels in largest white/black squares. The same logic shows that the smallest white/black retinal contrast is the ratio of the smallest, single pixel, retinal luminances. The results of the calculated retinal image show retinal luminance ratios from as high as 8.73 to 1 to as low as 1.16 to 1 (see Figure 7 and Table 2).

Another feature of retinal luminance images is the conversion of uniform *target luminance* to gradients of *retinal luminance*. The target was designed to have uniform patches of white and black squares. At each white/black edge, intraocular scatter transforms the sharp edge into a much smoother transition with a gradient. The slope of that gradient varies with the neighboring pixels. The simple uniform target luminances have been transformed into a very complex array of gradients. Figure 7 (center and right) shows the array of retinal luminances using colorbar =1.0. The retinal image is made of many complex gradients. The two different gray squares are very close in retinal luminance, in fact, they are indistinguishable in this rendering. There is no edge in the middle.

All white squares have identical target luminances, as do all black surround squares. However, both white and black squares have variable retinal luminances depending on the size of the square, as well as position in the surround. Constant target luminance does not ensure constant retinal luminance.

The retinal luminance image also shows that the largest squares (lowest spatial-frequency components) have the largest retinal luminance ratios. Nevertheless, the squares look the same whites and blacks. Regardless of the retinal luminances, the spatial processing mechanisms make the appearances the same. This suggests that different spatial frequency channels have different appearance outputs for constant retinal luminance inputs. Table 2 lists the target and retinal luminances for variable size white and black surround squares in Figure 7. The locations of the squares listed are shown in Figure 7 (right). The selection of these squares is arbitrary and does not represent any statistical analysis.

	DD white OD		DD black OD		W/B contrast OD	W/B edge ratio
Target	0.00		5.4		5.40	251,188.64
DD 64x	0.08		1.02		0.94	8.73
DD 32x	0.09		0.89		0.79	6.20
DD 16x	0.17		0.61		0.44	2.75
DD 8x	0.24		0.43		0.20	1.57
DD 4x	0.25		0.51		0.26	1.81
DD 2x	0.35		0.47		0.13	1.34
DD 1x	0.46		0.53		0.06	1.16

Table 2 lists the data and colormap rendering of white and black squares shown in Figure 7. The first column lists the areas sampled (Figure 7 right). The second (white) and fourth (black) columns list retinal luminance (OD). The third and fifth column show the colormap values for these densities. The sixth column lists the difference in OD. The last column lists the ratios of luminances from the center of the white and black squares. The second row shows the input target luminances for all squares. The remaining rows show typical output samples for retinal luminance in different size squares. The third through ninth rows show sample values for the largest square (64x) through the smallest square (1x). Retinal luminance values vary considerably with the surrounding portion of the image. These are typical values identified in Figure 7. The size of white and black squares has considerable influence on the retinal luminance, contrast and white/black (W/B) ratios.

Table 2 shows the relative optical densities of retinal luminances for different size white/black pairs. It shows the colorbar rendering of these luminances. It lists the difference in OD, and the ratio of retinal luminances at the centers of the square.

The final topic is the appearance of the white/black surround patches. Do they appear to have variable contrast as implied by their retinal luminance? Do they appear the same white and black for all sizes of squares? Although not measured experimentally with multiple observers and multiple trials, we observed that the white/black contrast appears the same regardless of the size of the white/black squares. Intraocular scatter controls the range of retinal luminance, which in turn controls the range of usable display dynamic range. The rate of change of white/black appearance scales varies with the amount of white in the surround.[15-18] The mechanism responsible for simultaneous contrast makes smaller retinal-luminance ratios appear more different. We have the paradox that lower retinal contrast generates higher apparent contrast.

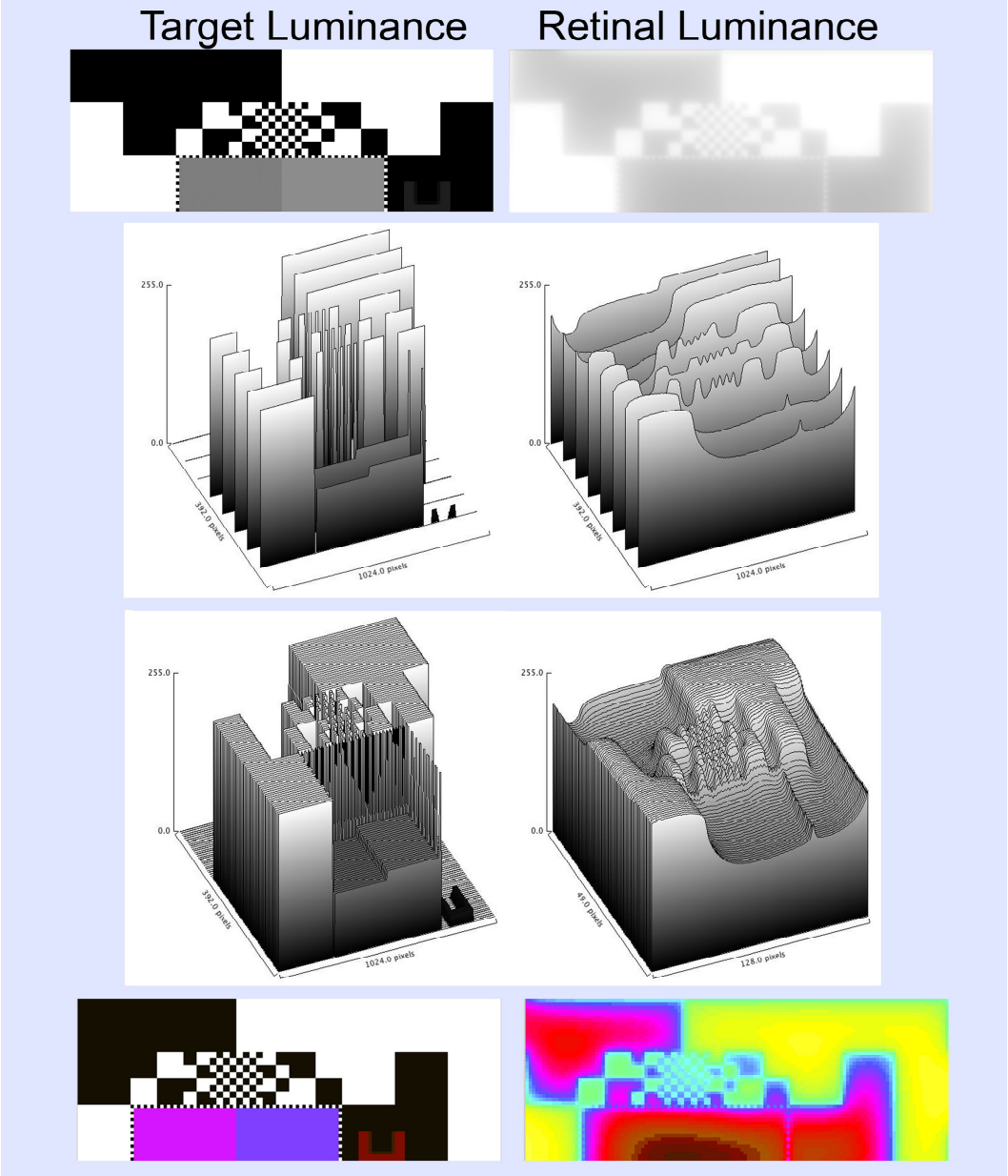

Figure 8 compares target luminances (left) with retinal luminances (right), for a portion of the image in section H. These comparisons use different scales for the left and right columns. In order to represent the 5.4 log units of target luminances(left) min/max ranges cover 5.4 OD, while the retinal luminances(right) min/max ranges cover 256:1, or 2.4 OD. The right column displays calculated luminance values scales to maximum value of 255. The top row compares target and retinal luminances. The second pair of comparisons shows 8 horizontal plots of luminance. The next pair of surface plots show 100 luminance slices. The bottom pair is the pseudocolor map used in Figure 7. All plots show that the uniform high-dynamic-range [OD= 5.4] target is transformed by glare into a non-uniform low-dynamic-range retinal image. Of particular interest are size-dependent effects on white/black edges. While all whites have the same target luminances, their retinal values vary considerably with the size of the white area. The retinal values of the black squares vary with both size and position in the image. Each sharp white/black edge in the target is transformed into image dependent gradients in retinal luminance.

The study of the white/black edges in the variable square surrounds suggests that apparent contrast mechanisms vary with spatial-frequency channels. The calculated retinal luminance image shows that smallest squares (highest spatial-frequency components) have the smallest retinal luminance ratios. Figure 8 illustrates the significant effects of intraocular scatter on the retinal image. It shows one of 20 different pairs of gray squares and its surround in the Double-Density target. The gray squares sections have different transmissions near 2.7 OD. All sizes of white squares have OD 0.0 and all blacks had 5.4 OD.

Since the dynamic ranges of target and retinal luminances are so different, we used different scaling to display the data. In Figure 8 the left column [target] shows the display luminance ODs over a range of 5.4 log units. The right column shows linear calculated retinal luminances (scaled max= 255).

Figure 8 uses four different visualizations to compare target and retinal luminances: scaled luminance, eight horizontal luminance plots, surface plots of luminance, and pseudocolor. Intraocular scatter transforms high-dynamic-range, uniform, constant square targets (left) into low-dynamic-range gradients with variable retinal luminance (right).

Human spatial-image-processing transforms this complex retinal image so that all "target whites" appear the same white and all "target blacks" appear the same black. HDR image processing techniques that attempt to mimic human vision need to differentiate the *optical* effects of intraocular glare from the *neural* spatial-image processing. Both optical and neural mechanisms show significant scene-dependent alteration of the image. These different image-dependent processes tend to cancel each other, making their presence less obvious.[17-18]

Conclusions

We measured the target luminance at each pixel, and calculated the retinal luminance array using the CIE standard glare spread function. Intraocular glare reduced the high-dynamic-range of target luminances to much smaller ranges, depending on image content. These limited-range retinal images are consistent with data from observer discrimination experiments. Further, the calculations show that there is no simple relationship between the retinal luminance of a pixel and its appearance between white and black. Observers report that the appearances of white and black squares are constant and uniform, despite the fact that the retinal stimuli are variable and non-uniform. Human vision uses complex spatial-image-processing to calculate appearance from retinal luminance arrays.

References

[1] E. Reinhard, G. Ward, S. Pattanaik, P. Debevec, High Dynamic Range Imaging Acquisition, Display and Image-Based Lighting, (Elsevier, Morgan Kaufmann, Amsterdam, 2006) chap 6,.

[2] J. J. McCann, "Art Science and Appearance in HDR images", *J. Soc. Information Display*, vol. 15(9), 709-719, 2007.

[3] J.J. McCann and A. Rizzi, "Camera and visual veiling glare in HDR images", J. Soc. Information Display, vol. 15(9), 721-730 (2007).

[4] J. J. McCann and A. Rizzi, "Optical veiling glare limitations to in-camera scene radiance measurements", in ECVP 2006 Abstracts, Perception, Vol. 35. Supplement, p. 51, (2006).

[5] J. J. McCann and A. Rizzi, "Spatial Comparisons: The Antidote to Veiling Glare Limitations in HDR Images" in Proc ADEAC /SID&VESA, Atlanta, 155-158, (2006).

[6] J.J. McCann, A. Rizzi, "Limits of HDR Images: Image Capture and Image Display", IS&T/SID Color Imaging Conference, Scottsdale; *Late Breaking News section,* Scottsdale, November, (2006).

[7] J. J. McCann and A. Rizzi, "Veiling glare: the dynamic range limit of HDR images", in Human Vision and Electronic Imaging XII, eds. B. Rogowitz, T. Pappas, S. Daly, Proc. SPIE, Bellingham WA, 6492-41, (2007).

[8] J. J. McCann and A. Rizzi, "Spatial Comparisons: The Antidote to Veiling Glare Limitations in Image Capture and Display" Proc. IMQA 2007, Chiba, E-1, (2007).

[9] J. J. Vos and T. J. T. P. van den Berg, "CIE Research note 135/1, Disability Glare", ISBN 3 900 734 97 6 (1999).

[10] CIE, "146 CIE equations for disability glare", in 146/147: CIE Collection on Glare, (2002).

[11] T. J. T. P. van den Berg, "Analysis of Intraocular Straylight, Especially in Relation to Age", Optometry and Vision Science, 72, No 2, pp. 52-59, (1995).

[12] J. J. McCann, "Aperture and Object Mode Appearances in Images", in Human Vision and Electronic Imaging XII, eds. B. Rogowitz, T. Pappas, S. Daly, Proc. SPIE, Bellingham, WA, **6292-26**, (2007).

[13] J. J. McCann and A. Rizzi, "The Spatial Properties of Contrast', in Proc. IS&T/SID Color Imaging Conference, Scottsdale; 11, p. 51-58, (2003).

[14] D. J Tolhurst, Y. Tadmor, and T. Chao "Amplitude spectra of natural images", Ophthalm Physiol Opt, 12, pp 229-232. (1992).

[15] A. Rizzi, M. Pezzetti, J.J. McCann, "Measuring the visible range of High Dynamic Range Images", *ECVP07, European Conference on Visual Perception,* Arezzo, **36** ECVP Abstract Supplement, (2007).

[16] A. Rizzi, M. Pezzetti, J.J. McCann, "Glare-limited Appearances in HDR Images", Color Imaging Conference 2007, Albuquerque (New Mexico), November 5-9, 2007.

[17] A. Rizzi, M. Pezzetti, J. J. McCann, "Separating the effects of glare from simultaneous contrast", paper in SPIE/IS&T Electronic Imaging Meeting, San Jose, 6806-09 January, (2008).

[18] J. J. McCann and A. Rizzi, "Appearance of High-Dynamic Range Images in a Uniform Lightness Space", *Proc. CGIV 08/IS&T, 4th European Conference on Colour in Graphics*, Terrassa, Spain, (2008).

Author Biography

John McCann (1964 AB. Degree, Biology, Harvard) worked in and managed, the Vision Research Laboratory, Polaroid (1961-1996). His 120 publications have studied Retinex theory, rod/Lcone color interactions at low light levels, appearance with scattered light, and HDR imaging. He is a Fellow IS&T, OSA; past President IS&T, Artists Foundation, Boston. He continues his research on color vision. He received the SID Certificate of Commendation, IS&T/OSA 2002 Edwin H. Land Medal, IS&T Honorary Member.

Alessandro Rizzi took degree in Computer Science at University of Milano and PhD in Information Engineering at University of Brescia. Now he is assistant professor, and senior research fellow at the Department of Information Technologies at University of Milano. Since 1990 he is researching in the field of digital imaging and vision. His main research topic is color information with particular attention to color perception mechanisms. He is the coordinator of the Italian Color Group.